Thermochimica Acta, 76 (1984) 287–300
Elsevier Science Publishers B.V., Amsterdam – Printed in The Netherlands

DIFFUSIONAL STUDY OF THE REACTION OF SULFUR DIOXIDE WITH REACTIVE POROUS MATRICES

TEVFIK BARDAKCI

Department of Chemical Engineering and Materials Science, The Catholic University of America, Washington, DC 20064 (U.S.A.)

(Received 15 November 1983)

ABSTRACT

A single-pellet high-temperature diffusion cell reactor is used to study the sulfation of calcined Greer limestone pellets. The effective diffusivities of gases through the reactive pellets, during the calcination and sulfation are determined. The experimentally determined effective diffusivity of sulfur dioxide through the pores of the product shell is used in the modified expanding grain model to obtain the diffusivity of sulfur dioxide through the product shell of the grains as a function of the conversion and the reaction temperature. The activation energy for the initial diffusivity of sulfur dioxide through the product shell of grains, is found to be 34.13 kcal mol^{-1}; the diffusivity values decreased with increasing conversion. Additionally it is found that the ratio of the tortuosity of reacting shell of pellet to the initial pellet tortuosity before any sulfation was increased with increasing conversion.

INTRODUCTION

It is important to control potentially harmful sulfur dioxide emitted into atmosphere by the combustion of fossil fuels. One of the developing technologies of sulfur dioxide removal is its reaction with calcined limestone in a fluidized bed combustor. The reaction of sulfur dioxide and oxygen within the reactive porous particles of lime has a complex nature. Borgwardt [1], who worked with precalcined dolomites and limestones, found that the reaction was first-order with respect to sulfur dioxide, and the rate of reaction decreased rapidly as the sulfation continued. Potter [2] and Borgwardt and Harvey [3] suggested that physical properties such as porosity, pore-size distribution, surface area and grain size of limestone play an important role during the reaction. Hartman and Coughlin [4] showed that both the porosity of the reacting particles and the sulfation reaction rate were decreased with increasing conversion.

There are numerous models for heterogeneous gas–solid reactions. Ramachandran and Doraiswamy [5] recently reviewed the various models. The grain model initiated by Szekely and co-workers [6–8] is useful for the

0040-6031/84/$03.00

modeling of heterogeneous gas–solid reactions. According to this model, a porous particle consists of spherical grains of uniform size separated by pores where the reacting gases diffuse; as the reaction proceeds, a shell of the reaction product which does not have any mass-transfer resistance, is formed on the grains. Pigford and Sliger [9] assumed that the reaction rate was governed either by the diffusion of sulfur dioxide through the pores or by its diffusion through the developing shells of the reaction product. Wen and Ishida [10] and Hartman and Coughlin [11] used similar models that accounted for sulfur dioxide diffusion in the porous particle. Hartman and Coughlin [11] considered the changes in the effective diffusivity of sulfur dioxide as a function of porosity change during the sulfation, but they neglected the changes in the tortuosity. They applied the shrinking-core model to each grain and considered a constant diffusion coefficient on the product layer of the grains. Hartman and Trnka [12], Georgakis et al. [13], and Garza-Garza and Dudukovic [14] considered the expanding grain size and the influence of temperature on the grain size, diffusion coefficients and the rate of reaction.

In this paper, the experimentally measured effective diffusivity of argon gas through the calcined pellet, as a function of the sulfation time is presented. These data were used to calculate the effective diffusivity of sulfur dioxide through the pores of the reacting shell of the pellet. The effective diffusivity of sulfur dioxide through the product shell of pellet was incorporated into the modified expanding-grain model to obtain the diffusivity of sulfur dioxide through the product shell of the grains as a function of the conversion and the reaction temperature. Also, the ratio of the tortuosity of the product shell to the initial tortuosity was calculated.

EXPERIMENTAL

A cylindrical pellet (typically 0.31-cm thick by 2.1-cm diameter) was manufactured using a diamond coring drill bit and a carborundum saw. The limestone used (Greer Limestone Co., Morgantown, WV) had an average calcium carbonate content of 75%. This pellet was mounted in a specially designed high-temperature diffusion cell, (Bardakci [15] and Bardakci and Gasner [16]), using the same principle as that of Wicke and Kallenbach [17]. The diffusion cell reactor was mounted in a tube furnace which was kept at a selected fixed temperature. Argon gas flowed radially across one face of the pellet while nitrogen gas flowed radially across the other face. The temperature was measured at each pellet face. The differential pressure between the two sides of the pellet was maintained at 0.00 ± 0.08 cm of water by computer control. The computer also measured and controlled flow rates and absolute pressures of each stream. In addition, it automatically injected samples from each stream into a gas chromatograph, integrated the output

and performed calculations including the effective diffusivity of argon and nitrogen through the reactive microporous pellet. After the complete calcination and some sintering of Greer limestone, the sulfation was started. During the sulfation pure nitrogen gas was passed over one side of the pellet. A special gas mixture which consisted of 1% O_2 and 500 ppm SO_2 in argon was passed over the other side of the pellet. The exit gas SO_2 concentration was measured continuously with a TECO Pulsed Fluorescent SO_2 Analyser (model 40).

The inlet SO_2 concentration was fixed; there was no SO_2 on the nitrogen side of the pellet. Using the fixed gas-flow rate and inlet and exit SO_2 concentrations a mass balance for SO_2 was performed to calculate the extent of the sulfation. At the end of each experiment the surface area of the unreacted portion of each pellet was measured with a Quantachrome Monosorb Surface Area Analyser (model MS-4). Samples taken from the reaction surface of each pellet were analyzed to determine the maximum saturation conversion.

THEORY

The Greer limestone pellets were fully calcined before the sulfation reaction. Mass transfer resistance to the external surface of the pellet was eliminated using high gas-flow rates. The following assumptions were taken:

(1) a porous cylindrical particle of lime is made up of a large number of uniform grains;

(2) temperature is uniform throughout the pellet;

(3) individual grains are sufficiently small for variations in gas concentrations on their surface to be negligible;

(4) the surroundings of the grains do not interfere with their growth;

(5) the pseudo-steady state approximation can be applied to this reaction system.

The material balance for SO_2 around the cylindrical pellet leads to the following equation

$$D_e \frac{d^2 C_{(x)}}{dx^2} - R = 0 \tag{1}$$

where

$$R = 3(1 - \epsilon_0) \frac{r_c^2}{(r_g')^3} k C_c \tag{2}$$

From the unreacted shrinking-core model for the concentration profile of sulfur dioxide in the product layer of the grain, the following equation can be derived

$$\frac{d^2C_1}{dr_1} + \frac{2}{r_1}\frac{dC_1}{dr_1} = 0 \tag{3}$$

with the boundary conditions

$$C_1 = C_{(x)} \text{ at } r_1 = r_g$$

$$D_s\left(\frac{dC_1}{dr_1}\right)_{r_1 = r_c} = kC_c \tag{4}$$

When eqn. (3) is integrated with the boundary conditions given in eqn. (4), the following expression is obtained

$$C_c = \frac{D_s C_{(x)}}{D_s + kr_c(1 - r_c/r_g)} \tag{5}$$

The rate at which the reaction interface moves may be expressed by

$$\frac{dr_c}{dt} = -\frac{k}{\rho_m}\frac{D_s C_{(x)}}{D_s + kr_c(1 - r_c/r_g)} \tag{6}$$

The boundary and the initial conditions for eqn. (1) are

$$\begin{aligned} C_{(x)} &= C_b \quad \text{at } x = 0 \\ C_{(x)} &= 0 \quad \text{at } x = L \end{aligned} \tag{7}$$

Those for eqn. (6) are given below

$$\begin{aligned} r_c &= r_g \quad \text{at } t = 0 \\ \frac{dr_c}{dt} &= 0 \quad \text{at } r_c = 0 \end{aligned} \tag{8}$$

The radius of the expanding grain as a function of local conversion is given by Hartman and Trnka [12]

$$r_g' = r_g\left\{1 - X_L\left[1 - \frac{\rho_{CO}}{\rho_{SP}}\left(1 + \frac{Y(M_{CS} - M_{CO})}{M_{CC} - Y(M_{CC} - M_{CO})}\right)\frac{1}{1 - \epsilon_{CS}}\right]\right\}^{1/3} \tag{9}$$

The local and overall conversions can be given as

$$X_L = 1 - r_c^3/r_g^3 \tag{10}$$

and

$$X_O = \frac{1}{L}\int_0^L (1 - r_c^3/r_g^3)\,dx \tag{11}$$

The porosity of the reacting particle of completely decomposed calcium carbonate is given by Hartman and Coughlin [4]

$$\epsilon_{(X)} = 1 - (1 - \epsilon_{LS})\left\{\rho_{LS}\frac{Y}{M_{CC}}[V_{CO} + X(V_{CS} - V_{CO})] - (1 - Y)\frac{\rho_{CC}}{\rho_{LS}}\right\} \tag{12}$$

The thickness of the product shell can be calculated as given below

$$l = LX_O/X_{sat} \tag{13}$$

Then the overall mass-transfer resistance can be obtained by addition of the mass-transfer resistances of the product shell and of the unreacted lime

$$\frac{L}{D_{eo}} = \frac{l}{D_e} + \frac{L-l}{D_{ei}} \tag{14}$$

From eqn. (14) D_e can be calculated

$$D_e = l/\{L/D_{eo} - [(L-l)/D_{ei}]\} \tag{15}$$

The initial grain radius is calculated from the following equation

$$r_g = \frac{3(1-\epsilon_0)}{S_g \rho_{CO}} \tag{16}$$

The coupled eqns. (1) and (6) were approximated by finite difference formulation and solved as a boundary value problem. The diffusivity of SO_2 through the grain product layer is difficult to measure. Thus, in order to obtain a better fit at higher conversion, it was varied as a function of conversion.

Calculation of tortuosity ratio

The effective overall diffusivity through the pellet before the sulfation reaction, can be given as

$$D_{ei} = D_0 \frac{\epsilon_0}{\tau_0} \tag{17}$$

During the sulfation, the effective diffusivity through the sulfated shell, at a given time, can be written as

$$D_e = D_0 \frac{\epsilon_l}{\tau_l} \tag{18}$$

The ratio of the tortuosities can be calculated from eqns. (17) and (18)

$$\frac{\tau_l}{\tau_0} = \frac{D_e}{D_{ei}} \frac{\epsilon_l}{\epsilon_0} \tag{19}$$

RESULTS AND DISCUSSION

From the measurements of the specific surface areas using eqn. (16) the initial grain radii were calculated. The calculated and reported (Hartman and Trnka [12] and Borgwardt and Harvey [3]) grain radii are presented in Fig. 1. The new values are between the previously reported values and they

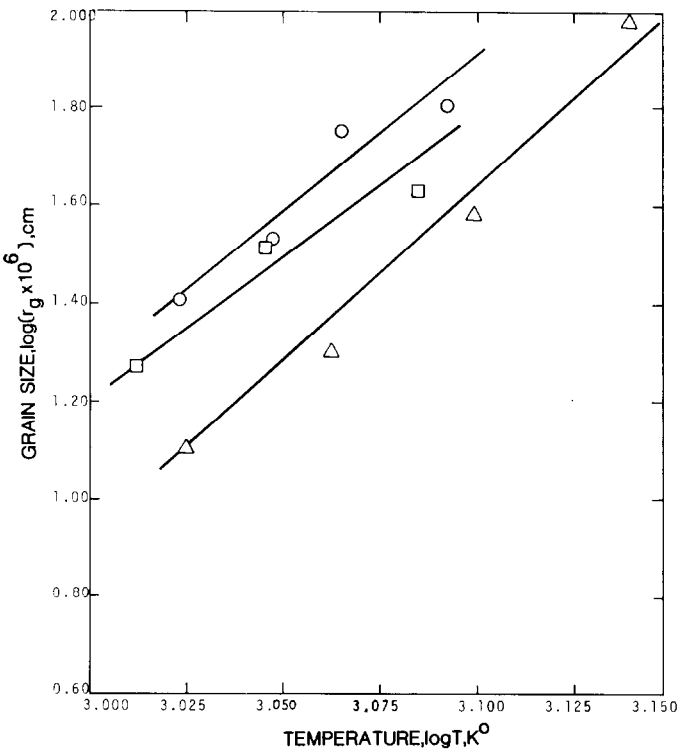

Fig. 1. Dependence of the initial grain size on calcination temperature. (○) Hartman and Trnka [12]; (△) Borgwardt and Harvey [3]; (□) present communication.

increase with increasing calcination temperature. The measured specific surface areas and the saturation conversions at the reacting pellet surface are given in Table 1. In Test R1, which was performed at 843°C, the NaCl salt vapor was passed over the pellet surface. Thus, it increased the ionic mobility and caused more sintering to give a low surface area conversely a high grain radius. The highest surface area was obtained at the lowest calcination temperature. At the end of Test R4 a sulfur map of the cross-section of the pellet was obtained using X-ray diffraction (see Fig. 2). The sulfation took place only on the right-hand side of the pellet where the reactant SO_2 gas

TABLE 1

Surface area and saturation conversion data

Test No.	Temp. (°C)	Surface area ($m^2\ g^{-1}$)	Saturated, % conversion
R1	843	2.41	0.4300
R2	942	2.24	0.4810
R3	756	5.45	0.2792
R4	840	3.14	0.4680

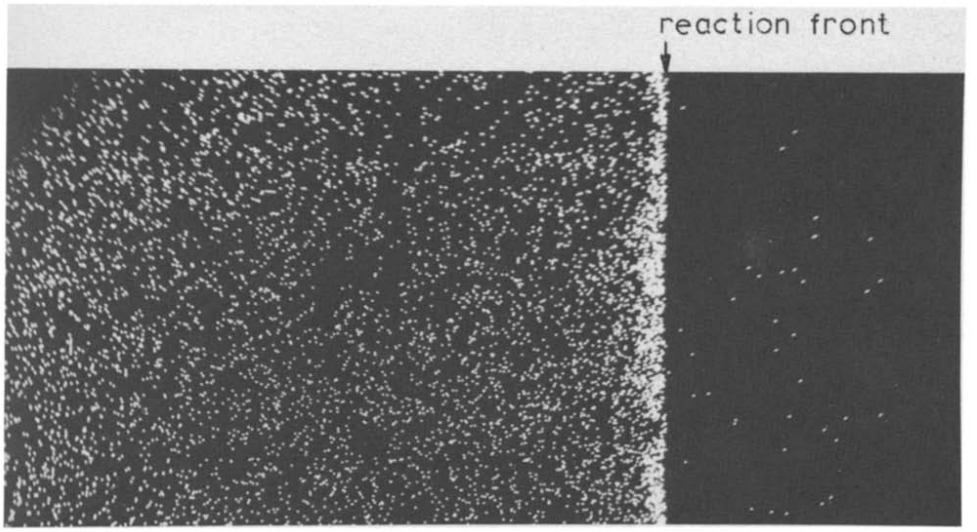

Fig. 2. Sulfur map of the cross section of the sulfated limestone (Test R4, 40×).

was in contact with the pellet surface. The background spots should be ignored in Fig. 2. A tortuous product shell was formed on the reaction side of the pellet. The changing effective diffusivity of sulfur dioxide through this thickening product shell was employed in the new modified grain model which was derived for a cylindrical pellet.

The measured effective diffusivity of argon during the sulfation tests are plotted as a function of sulfation time in Fig. 3. Using the inverse square root of molecular weight ratio relation given by Evans et al. [18] the overall

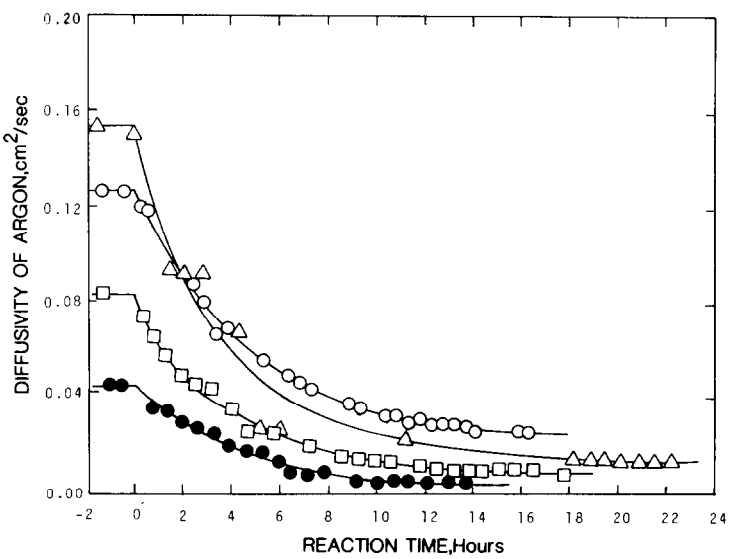

Fig. 3. Effective diffusivity of Ar as a function of reaction time. (○) 843°C; (△) 942°C; (□) 840°C; (●) 756°C.

effective diffusivity of sulfur dioxide was calculated. The effective diffusivity of SO_2 through the developing product shell which controls the sulfation reaction, was calculated using eqns. (13) and (15). The calculated values are plotted as a function of sulfation time and conversion in Figs. 4 and 5, respectively. The effective diffusivity through the product shell was decreased as the reaction time or conversion was increased. These effective diffusivity values of SO_2 through the product shell were used in the new model with the parameters shown in Table 2. The kinetic rate constants, which are the extrapolated values of the kinetic constants at 0 h of sulfation, were calculated assuming a first-order reaction with respect to SO_2 concentration. The diffusivity of SO_2 through the product shell of the grain,

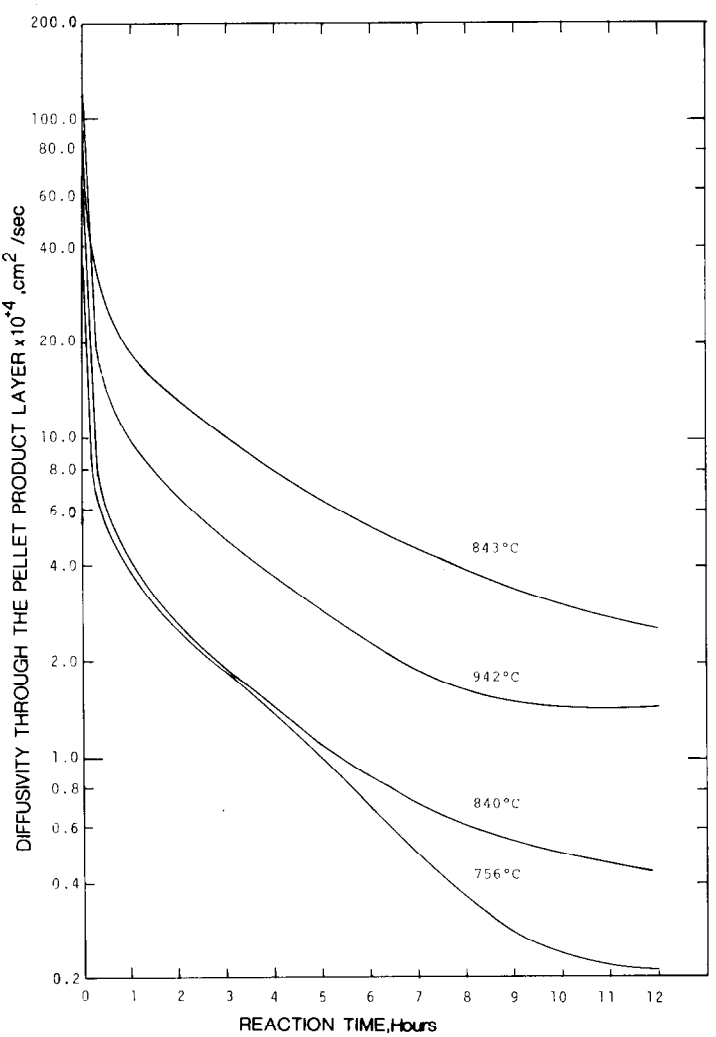

Fig. 4. Effective diffusivity of SO_2 through the pellet product layer vs. reaction time.

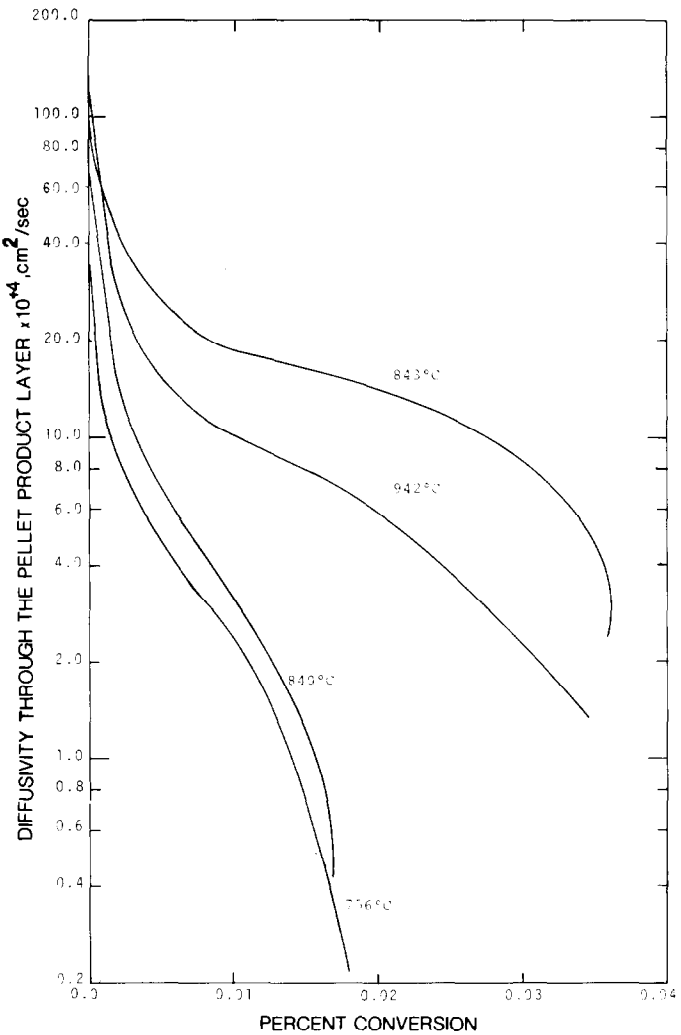

Fig. 5. Diffusivity through the pellet product layer vs. percent conversion.

which was varied with conversion in order to obtain a better fit at higher conversion, was the only parameter obtained through the model fitting.

The experimental and predicted conversion of calcined Greer Limestone to calcium sulfate are shown in Fig. 6. Since the NaCl salt vapor was passed through the pellet surface, a higher conversion was obtained during the test performed at 843°C. The diffusivity of SO_2 through the product shell of the grain, obtained by model fitting, are plotted as a function of conversion in Fig. 7. The diffusivities of SO_2 through the product shell of the grain were increased with increasing temperature and, at a fixed temperature, they decreased with increasing conversion. The latter is true, because with the grain expansion the length of the diffusion path within the grain is increased.

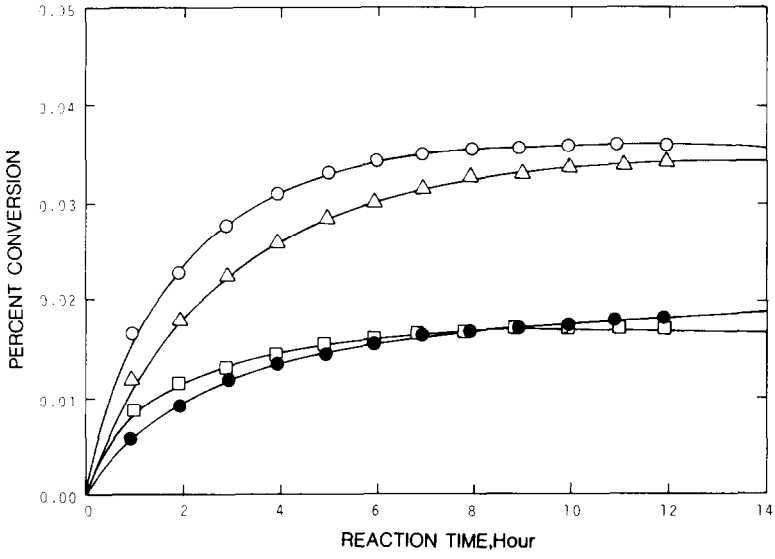

Fig. 6. Percent conversion as a function of reaction time. (○) 843°C; (△) 942°C; (□) 840°C; (●) 756°C; (————) corresponding model predictions.

After a certain conversion these diffusivity values decreased sharply, practically stopping the sulfation reaction. The initial values of this diffusivity are plotted in Fig. 8 with the values reported by Hartman and Trnka [12] as a function of $1/T$. The values found in this study are much smaller than the reported values. The equation below gives the initial diffusivity of SO_2 through the product shell of grains as a function of the absolute temperature

$$D_{si} = 4.20 \times 10^{-3} \exp(-34130/RT) \tag{20}$$

TABLE 2

Model parameters

	Test No.			
	R1	R2	R3	R4
Temperature (°C)	843	942	756	840
Inlet SO_2 conc. $\times 10^8$ (g mol cm^{-3})	2.2071	2.2480	2.2480	2.0763
Thickness of the pellet (cm)	0.3260	0.3295	0.3260	0.3168
Grain radius $\times 10^5$ (cm)	4.1	4.5	1.8	3.2
Reaction rate constant (cm s^{-1})	4.75	2.45	0.65	2.75
Effective diffusivity of SO_2 through shell of the pellet (cm^2 s^{-1})	(see Fig. 4)			
Diffusivity of SO_2 through the grain product (model fitted) (cm^2 s^{-1})	(see Fig.7)			

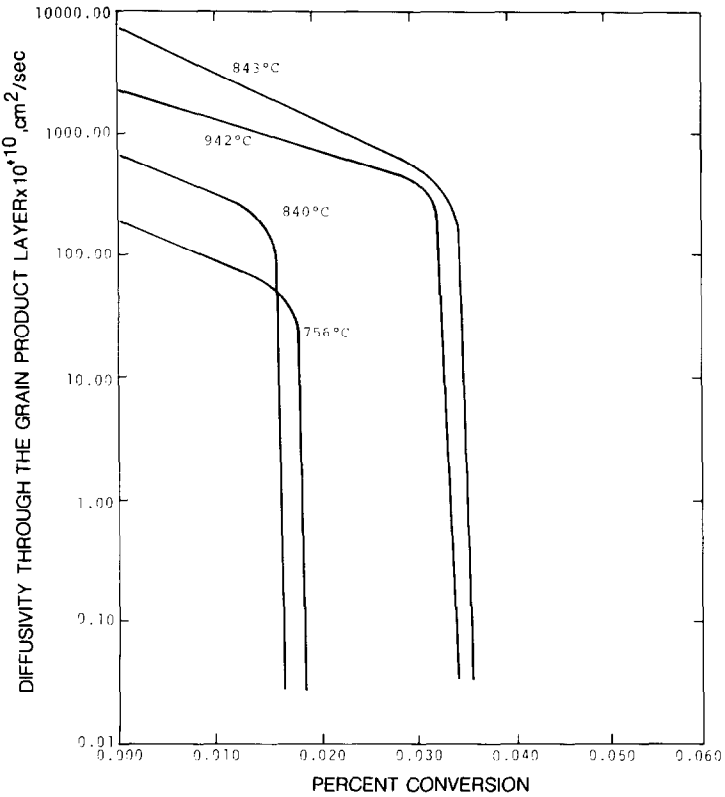

Fig. 7. Diffusivity through the grain product layer as a function of percent conversion.

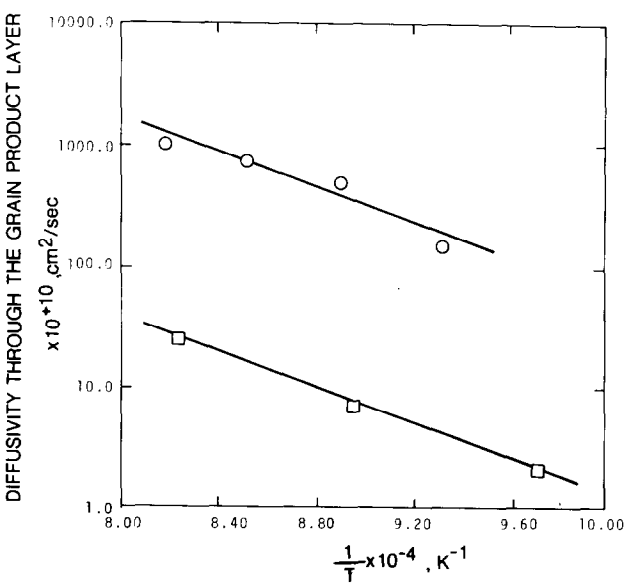

Fig. 8. Initial diffusivity through the grain product layer vs. $1/T$. (○) Hartman and Trnka [12]; (□) present communication.

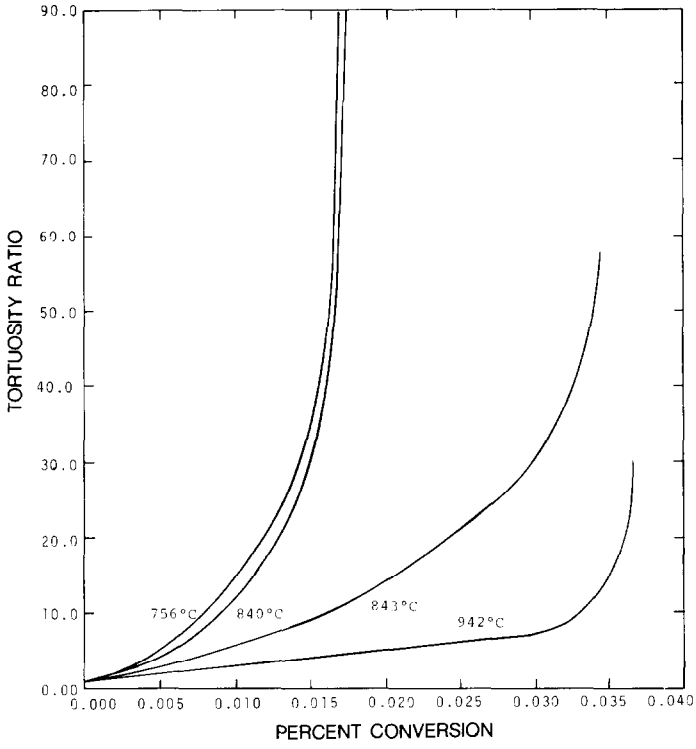

Fig. 9. Tortuosity ratio vs. percent conversion.

The result of Test R1 is not included in eqn. (20) since the salt vapor was added before the experiment. The activation energy of 34.13 kcal mol^{-1} is very close to its experimentally determined value of 35.6 kcal mol^{-1} reported by Marsh and Ulrichson [19].

In a different set of calculations the ratio of tortuosity of reacting product shell of the pellet to the initial tortuosity of pellet before any sulfation was determined using eqns. (12), (13), (15) and (19). The tortuosity ratio was plotted as a function of conversion in Fig. 9. This ratio was increased with increasing conversion, and higher values were obtained at lower temperatures. The salt vapor also slowed this increment.

CONCLUSION

During the sulfation of a porous pellet, a tortuous product shell develops. Therefore, the effective diffusivity of sulfur dioxide through the product shell decreased with an increase in conversion or sulfation time. The diffusivity of sulfur dioxide through the grains also decreased with increasing conversion. The activation energy for this diffusion was found to be 34.13 kcal mol^{-1}.

Contrary to the previous assumptions the tortuosity of the reaction shell is not constant. The tortuosity increased as the sulfation reaction progressed.

LIST OF SYMBOLS

C_b bulk concentration of SO_2 (mol cm^{-3})
C_c concentration of SO_2 at reaction interface of grain (mol cm^{-3})
C_l concentration of SO_2 within product shell of grain (mol cm^{-3})
$C_{(x)}$ concentration of SO_2 within pores as a function of the distance from reacting pellet surface (mol cm^{-3})
D_e effective diffusivity of SO_2 through product shell of pellet during the reaction, defined by eqn. (15) ($cm^2\ s^{-1}$)
D_{ei} effective diffusivity of SO_2 before sulfation ($cm^2\ s^{-1}$)
D_{eo} overall effective diffusivity of SO_2 at any time ($cm^2\ s^{-1}$)
D_o diffusion coefficient of SO_2 in pores ($cm^2\ s^{-1}$)
D_s diffusivity of SO_2 through product of grain ($cm^2\ s^{-1}$)
D_{si} initial diffusivity of SO_2 through product shell of grain ($cm^2\ s^{-1}$)
k chemical reaction rate constant (cm s^{-1})
l shell thickness (cm)
L length of pellet (cm)
M_j molecular weight (g mol^{-1})
R defined by eqn. (2)
r_c radius of unreacted part of the grain (cm)
r_g initial radius of grain (cm)
r_g' radius of expanded grain (cm)
r_l radial coordinate within product shell of grain (cm)
S_g BET surface area ($cm^2\ g^{-1}$)
t time of exposure of SO_2 to pellet (s)
T reaction temperature (K)
V_j molar volume of pure component ($cm^3\ mol^{-1}$)
x distance from reacting pellet surface (cm)
X conversion of calcium oxide to calcium sulfate
X_L local conversion of calcium oxide to calcium sulfate, defined by eqn. (10)
X_O overall conversion of calcium oxide to calcium sulfate, defined by eqn. (11)
X_{sat} saturation conversion of calcium oxide to calcium sulfate at the pellet surface
Y content of calcium carbonate in limestone, weight fraction

Greek letters

ϵ porosity
ϵ_0 initial porosity of calcined limestone

ϵ_t porosity of calcined pellet during the sulfation at time t
ρ_j density (g cm^{-3})
ρ_m molar calcium oxide density of grain (g mol cm^{-3})
τ_0 tortuosity of fully calcined limestone before sulfation
τ_t tortuosity of pellet during sulfation time (t)

Subscripts

CC calcium carbonate
CO calcium oxide
CS calcium sulfate
LS limestone
SP solid reaction product

ACKNOWLEDGMENT

The author thanks Dr. L.L. Gasner and M. Kaya for helpful discussions.

REFERENCES

1 R.H. Borgwardt, Environ. Sci. Technol., 4 (1970) 59.
2 A.E. Potter, Am. Ceram. Soc. Bull., 48 (1969) 855.
3 R.H. Borgwardt and R.D. Harvey, Environ. Sci. Technol., 6 (1972) 350.
4 M. Hartman and R.W. Coughlin, Ind. Eng. Chem. Process Des. Dev., 13 (1974) 248.
5 P.A. Ramachandran and L.K. Doraiswamy, AIChE J., 28 (1982) 881.
6 J. Szekely and T.W. Evans, Chem. Eng. Sci., 25 (1970) 1091.
7 J. Szekely and T.W. Evans, Chem. Eng. Sci., 26 (1971) 1901.
8 H.Y. Sohn and J. Szekely, Chem. Eng. Sci., 29 (1974) 630.
9 R.L. Pigford and G. Sliger, Ind. Eng. Chem. Process Des. Dev., 12 (1973) 85.
10 C.Y. Wen and M. Ishida, Environ. Sci. Technol., 7 (1973) 703.
11 M. Hartman and R.W. Coughlin, AIChE J., 22 (1976) 490.
12 M. Hartman and O. Trnka, Chem. Eng. Sci., 35 (1980) 1189.
13 C. Georgakis, C.W. Chang and J. Szekely, Chem. Eng. Sci., 34 (1979) 1072.
14 O. Garza-Garza and M.P. Dudukovic, Chem. Eng. J., 24 (1982) 35.
15 T. Bardakci, Ph.D. Thesis, University of Maryland, College Park, MD, May 1980.
16 T. Bardakci and L.L. Gasner, Thermochim. Acta, 45 (1981) 233.
17 E. Wicke and R. Kallenbach, Kolloid-Z., 97 (1941) 135.
18 R.B. Evans, G.M. Watson and E.A. Mason, J. Chem. Phys., 35 (1961) 2076.
19 D.W. Marsh and D.L. Ulrichson, Annual AIChE Meeting, Los Angeles, CA, November, 1982, Pap. 56C.